J. Fluid Mech. (1996), *vol.* 308, *pp.* 171–194

Concerning marginal singularities in the boundary-layer flow on a downstream-moving surface

By S. N. TIMOSHIN

Department of Mathematics, University College London, Gower Street, London WC1E 6BT, UK
and Central Aerohydrodynamical Institute, Zhukovsky, Russia, 140160

(Received 19 September 1994 and in revised form 23 August 1995)

The formation of separation singularities in solutions of the classical boundary-layer equations is studied numerically and analytically for the case of a two-dimensional incompressible steady flow near a solid surface moving in the direction of the main stream. Unlike the previously studied regime of the incipient separation located at the maximum point in the external pressure distribution, the breakdown in this work occurs under an adverse pressure forcing and involves a regular flow field upstream of the Moore–Rott–Sears point with an algebraic non-analyticity downstream. Small deviations from the precisely regular approach to the singular point are shown to result in an exponential amplification of linear disturbances; in the subsequent nonlinear stage the solution terminates in a finite-distance blow-up singularity or, alternatively, continues in a regular fashion across the singular station. The case of asymptotically small slip velocities is considered and a connection with marginal separation on a fixed wall is discussed.

1. Introduction

Studies of laminar boundary layers on moving surfaces have several main areas of application including, most notably, flow control and optimization, see e.g. Chang (1976), and unsteady separation, Williams (1977) and Sychev *et al.* (1987). Related problems also arise in calculations of the time-average flow around vibrating bodies at large values of the 'oscillatory' Reynolds number as described e.g. in Stuart (1963) and Riley (1975), especially in the regime of interaction between the incoming and induced mean-flow components (Timoshin 1988), and in recent investigations of nonlinear instabilities in wall-confined flows; see Smith & Walton (1989), Walton & Smith (1992). The concern of the present paper is with the origin of a singular behaviour in solutions of the Prandtl boundary-layer equations for a two-dimensional incompressible steady flow on a downstream-moving surface. It has been known since the numerical work of Telionis & Werle (1973) that, subject to an adverse pressure gradient, a boundary layer of this type can develop a strong blow-up singularity at the position of the first appearance of reversed flow in the middle of the streamwise velocity profile, in accord with the Moore–Rott–Sears (*MRS*) criterion of separation; see e.g. Telionis (1981). The local analytic structure of the singularity was uncovered later by Sychev (1980) and Elliott, Smith & Cowley (1983). It is widely recognized now that practical implications of the singular termination of the flow at separation in this and in many other examples of the Prandtl formulation with a prescribed

pressure depend on the particular physical situation and can be dramatic in view of the often inevitable global separation of the boundary layer in such cases, with immediate impact on the stability of the flow, drag, performance of the airfoil, etc; for a discussion and further references see e.g. Stewartson (1974), Smith (1982*a*) and Sychev *et al.* (1987).

In this work we are interested in the nature of an intermediate, marginal state of the boundary layer bordering the regimes of smooth, attached and grossly separated flows. In the framework of the Prandtl strategy the incipient separation can be naturally attributed to the formation of mild isolated singularities in the solution of the boundary-layer equations, with the flow well-behaved and forward both upstream and downstream of the critical station. In realistic situations the marginal singularity can emerge, for example, in an initially regular flow field as a result of parametric changes in the flow conditions and, therefore, knowledge of the circumstances accompanying the origin of separation is important in evaluating the parameter range for the validity of the boundary-layer approach and, more generally, for the relevance of the expected or assumed structure of the flow as a whole.

The theory for the flow on a fixed wall was developed by Ruban (1981, 1982*a*) and Stewartson, Smith & Kaups (1982), applied to boundary-layer separation on the rounded leading edge of an airfoil at incidence; further developments in this area are summarized in the review articles by Smith (1982*a*, 1986) and Ruban (1990). The theory showed that, depending on the value of the angle of attack of the airfoil α, the solution of the boundary-layer equations either remains regular on the entire leading edge, when $\alpha < \alpha_c$ say, or develops the Goldstein (1948) singularity at a finite distance from the front stagnation point when $\alpha > \alpha_c$. In the marginal regime, $\alpha = \alpha_c$, the flow is regular and forward up to the point of vanishing skin friction, and admits a two-fold (at least) extension further downstream. The first possibility is an analytic continuation of the regular solution into the domain of reversed flows. Exponentially weak non-analyticity associated with the upstream propagation of disturbances (or the inverse parabolicity of the equations of motion) introduces further non-uniquenesses in the reversed-flow regular branch, see Stewartson (1958) and Smith (1984). The second, and a less obvious possibility incorporates a forward-flow solution with a discontinuous gradient of the streamfunction. It is this second solution that provides the limiting state of the boundary layer when the angle of attack approaches α_c from below. The concept of a marginal singularity on a fixed wall proves crucial for understanding the hysteresis and stall phenomena in flows near turbine blades and aircraft wings; see the references above.

The issue of a marginal singularity on a downstream moving surface was first raised by Sychev (1987) in connection with the flow separation on a rapidly rotating cylinder immersed in a uniform stream. In agreement with computations by Nikolayev (1982), the Sychev theory rests on the assumption that the position of the incipient singularity coincides with the maximum point in the external pressure distribution. When the angular velocity of rotation decreases to a certain finite value the boundary-layer thickness on the cylinder develops a gradually growing isolated maximum accompanied by the formation of the *MRS* point in the velocity profile tangential to the surface. According to Sychev (1987), the singularity originates in a locally inviscid, pressure-driven deceleration of the fluid particles in the middle layers of the flow upstream of the critical section followed by a predominantly symmetric (owing to the effective lack of viscous diffusion) acceleration immediately downstream. More recent computations carried out by Lam (1988) confirmed the trend towards the unbounded thickening of the boundary layer on approach to the critical state, as well

as the choice for the position of the singularity at the point of zero pressure gradient. It is interesting, however, that the numerical solution does not seem to reproduce the theoretically expected shape of the velocity profile in the vicinity of the *MRS* point, an issue which requires further computations.

The rotating cylinder provides an important but, at the same time, a very special example of the moving-wall boundary layer. For the flow, apart from being singular in one particular section, must also be periodic in the angular coordinate, a condition which imposes severe restrictions on the class of admissible solutions and on the form of singularity, we believe. Again, the requirement of zero pressure gradient at or close to the incipient breakdown does not seem to be universal on physical grounds, especially bearing in mind the fixed-wall singularity which first appears in the region of a decelerating external forcing.

In the subsequent sections of this paper we aim to show that a marginal singularity in the moving-wall flow is indeed possible under an adverse pressure gradient, in which case properties of the local solution are bound to be new, different from those in Sychev (1987). First, in our analysis the marginal structure is viscosity-dominated both upstream and downstream of the critical section where the *MRS* conditions are first met. Secondly, and rather surprisingly (although not dissimilar from the case of the fixed-wall boundary layer), the flow field turns out to be completely *regular* in its upstream part up to the *MRS* section, and continues downstream with an algebraic singularity in the displacement thickness and an infinite gradient of the streamfunction. The third main feature of the solution will be seen in the manner in which the marginal structure responds to infinitesimal changes in the initial and boundary conditions introduced far upstream. The reaction of the flow at the regular *MRS* point to stationary disturbances is found to be based on exponential eigenfunctions locally, and, therefore, the response is much stronger than in the fixed-wall case, cf. Ruban (1981, 1982*a*) and Stewartson *et al.* (1982). This feature has immediate connections with the mechanism of the usual temporal instability which operates in any classical boundary layer with non-monotonic velocity profiles (see Cowley, Hocking & Tutty 1985); the relation between the temporal mode and the stationary eigenfunction is discussed in Timoshin (1995). The fourth, and the final new property to be mentioned here, follows directly from the nature of the local eigenfunction in the linearly perturbed flow. Subject to small disturbances the marginal solution undergoes local, nonlinear and viscous, transformations somewhat upstream of the singular point and then terminates with a strong blow-up singularity of the Sychev (1980) or Elliott *et al.* (1983) variety, or, alternatively, continues smoothly into the region of accelerating flows. This explains the significance of the marginal solution in dividing the fully regular attached and strongly singular separated regimes of the boundary-layer development.

Various arguments are summoned in order to demonstrate the existence and, more importantly, the typicality of marginal separation with the properties listed. So, §2 deals with the numerical solution for a model situation involving the development of a constant-shear flow affected by an adverse pressure gradient. Despite its simplicity and model nature, the problem provides a physically realistic example of the flow in the lower part of a conventional, e.g. Blasius, boundary layer on a fixed wall altered by a localized disturbance in the external pressure, cf. Smith *et al.* (1981), with a slip velocity applied simultaneously at the wall. We show that for a fixed slip velocity flow separation tends to develop when the pressure forcing reaches a certain level; the form of the singularity at separation supports the suggested regular approach to the *MRS* point. The major properties of the marginal solution, including the singular

continuation downstream, linear eigenfunctions and the nonlinear bifurcation are addressed in §3 in a local consideration in a small vicinity of the regular *MRS* point. The case of a small slip velocity and a connection with the wall singularity on a fixed surface are examined in §4. The paper concludes with a brief discussion of the results and of possible extensions of this work.

2. Numerical solution of a model problem

The boundary-layer flow of an incompressible fluid on a moving surface is governed by the equation

$$\frac{\partial\psi}{\partial y}\frac{\partial^2\psi}{\partial x\partial y}-\frac{\partial\psi}{\partial x}\frac{\partial^2\psi}{\partial y^2}+p'(x)=\frac{\partial^3\psi}{\partial y^3} \tag{2.1}$$

for the non-dimensional streamfunction $\psi(x,y)$, with the boundary conditions

$$\psi=0, \quad \partial\psi/\partial y=\delta u_w(x) \quad \text{at} \quad y=0. \tag{2.2}$$

Here x, y denote the non-dimensional coordinates along and normal to the surface respectively; the pressure gradient $p'(x)$ and the slip velocity $\delta u_w(x)$ are assumed to be given and δ is a parameter. Equation (2.1) also requires a boundary condition at the outer edge of the boundary layer as $y\to\infty$, and an initial condition at $x=0$, say. These depend largely on the particular flow geometry.

In the model problem considered in this section an infinitely long flat plate moves along the x-axis with a constant velocity δ, so that $u_w=1$ in (2.2); the flow is in the half-plane $y\geqslant 0$. In the domain $x\leqslant 0$, the pressure and the vorticity are assumed to be constant, and then the streamfunction is written as $\psi=y^2/2+\delta y$, after a suitable normalization. The flow downstream of the origin is affected by a prescribed pressure gradient. Hence equation (2.1) is to be solved in the domain $x\geqslant 0$, $y\geqslant 0$ with the boundary conditions (2.2), with the initial condition

$$\psi=\tfrac{1}{2}y^2+\delta y \quad \text{at} \quad x=0, \ y\geqslant 0, \tag{2.3}$$

and subject to the outer-edge constraint

$$\psi=\tfrac{1}{2}(y-\Delta(x))^2+p(x)-\tfrac{1}{2}\delta^2+o(1) \quad \text{as} \quad y\to\infty, \tag{2.4}$$

containing the displacement function $\Delta(x)$ unknown in advance.

The formulation (2.1)–(2.4) is typical for a boundary layer of the conventional (e.g. Blasius) type encountering sudden changes in the flow conditions such as for instance a relatively short and shallow roughness on the wall, cf. Smith *et al.* (1981). The crucial local responce in the perturbed flow is concentrated then in the lowest part of the main boundary layer; therefore only a constant-shear part of the basic-state velocity profile is retained in the initial/boundary conditions for the disturbance. Here we suppose (and verify in the subsequent sections) that the nature of the breakdown in the moving-wall problem is mostly independent of the particular outer-edge constraints. The next significant point in our modelling is a convenient choice for the driving pressure gradient in (2.1). In the incompressible-flow theory the pressure is determined by the roughness shape via the Cauchy–Hilbert integral of a thin-airfoil kind or, alternatively, the appropriate roughness can be found as an improper integral of a chosen pressure gradient. However, in order to deal with realistic body shapes (especially when the pressure is assumed constant upstream of a certain station as in (2.5) below) and also to achieve a better control over the properties of the pressure distribution, we shall now take a broader view on the physical origin of the local

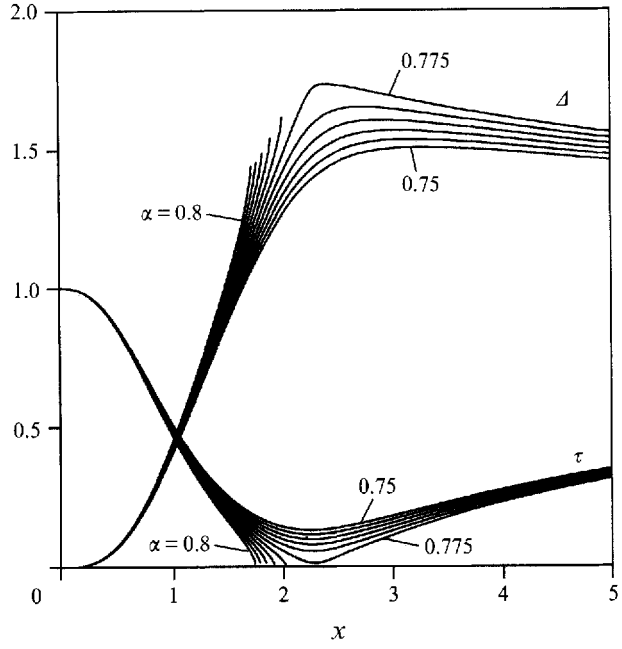

FIGURE 1. The skin friction τ and the displacement thickness Δ *vs.* x for a fixed-wall flow, $\delta = 0$, from numerical solution of (2.1)–(2.5). The curves are drawn with the step $\Delta\alpha = 0.005$.

problem and include in the scope of the theory other basic flows such as compressible boundary layers (both subsonic and supersonic, up to high Mach numbers), viscous wall jets, liquid films, and so on. The perturbed-flow formulation for all of them reduces to (2.1)–(2.4) in effect (e.g. Smith 1982*a*; Sychev *et al.* 1987; Timoshin & Smith 1995), with the global flow arrangement being only reflected in the form of the pressure/roughness-shape link. The latter proves to be remarkably simple in certain cases. So for a supersonic outer flow the Ackeret formula shows that the roughness height is proportional to an integral of the pressure, hence a sensible body shape is obtained for virtually any given forcing. In the case of a wall-jet boundary layer the shape is related to a double integral of the pressure function. Or, even simpler, a direct pressure–height proportionality holds for certain regimes of perturbed liquid films. Each of these flow configurations may be looked at as providing a realistic background for our analysis in this section where the pressure forcing rather than the underlying local disturbance source is specified explicitly.

In the computations below the pressure gradient is chosen in the form

$$p'(x) = \alpha x^2 \left(1 + x^3\right)^{-1} \quad \text{for} \quad x > 0; \quad p'(x) \equiv 0 \quad \text{for} \quad x < 0, \tag{2.5}$$

which, with a variable amplitude parameter $\alpha > 0$, features a very mild adverse forcing at both small and large distances downstream with the maximum $p'_{max} = 2^{2/3}\alpha/3$ at $x = 2^{1/3}$. The initial and boundary-value formulation (2.1)–(2.5) was then solved numerically with an implicit second-order-accurate in x and y method, marching in the positive x-direction with iterations at each step. The outer-edge condition (2.4) in the form $\partial^2\psi/\partial y^2 = 1$ was imposed at a suitably large distance $y = y_{max}$ from the wall.

The flow on a fixed wall ($\delta = 0$) provides a convenient test of the relevance of the model. The computed distributions of the skin friction $\tau(x) = \partial^2\psi/\partial y^2\,(y = 0)$ and

of the displacement thickness $\Delta(x)$ are shown in figure 1 for a few values of α near $\alpha_c \approx 0.775$ which marks the cross-over from the regular flow to the Goldstein-type breakdown with a square-root singularity in the wall shear. The marginal singularity develops at approximately $x_s = 2.29$. The computational grid in this example has $y_{max} = 8$ and the step lengths $\Delta x = 0.00625, \Delta y = 0.005$.

Our main computations were for two values of the wall velocity, $\delta = 0.1$ and $\delta = 0.2$, and variable pressure forcing. The typical grid parameters are $\Delta x = 0.00625, \Delta y = 0.0025, y_{max} = 8$, although in the case $\delta = 0.2$ we found it necessary to increase y_{max} to 16 in order to preserve the accuracy of the displacement function. We observe, first of all, that the slip effect postpones the flow separation to a certain extent, so that the solution remains regular in the α-range up to approximately $\alpha_c = 0.893$ for $\delta = 0.1$ and then up to $\alpha_c = 1.014$ for $\delta = 0.2$. However, further increase in the pressure forcing leads in both cases to the formation of a new marginal state and, subsequently, to a singular breakdown of the flow. The skin-friction and the displacement thickness distributions shown with solid lines in figure 2(*a*) for the first case $\delta = 0.1$ split up into two distinct groups. The singular solutions ($\alpha > \alpha_c$) terminate with an abrupt thickening of the boundary layer. The singularity is very strong and, owing to its development within a relatively short x-interval, it is difficult to obtain accurate solutions closer to the breakdown without excessive grid refinement although the behaviour of the displacement thickness and the formation of a pronounced minimum, tending to zero, in the streamwise velocity profiles (not shown in the graph) indicate the locally inviscid internal singularity studied in Sychev (1980) and Elliott *et al.* (1983).

The family of regular solutions for a somewhat lower pressure gradient in figure 2(*a*) reveals the tendency to build up a distinct maximum in the displacement thickness as α increases to its critical limit. The thickening of the boundary layer is clearly due to a local deceleration of fluid particles in the middle of the flow. In the subcritical regime the deceleration is followed by a sudden acceleration (regardless of the overall adverse forcing) with the displacement thickness simultaneously decreasing. Qualitatively, the process is similar to the behaviour of fluid particles in the near-wall layers on the fixed surface, cf. figure 1, and also resembles the formation of the singularity in the rotating-cylinder problem although, in contrast to the latter case, the maximum displacement seems to be finite in the limit and the flow functions become strongly asymmetric near to the breakdown.

Next an attempt was made to approach closer to the incipient separation using the technique of parametric shooting with refinement of the α-interval between the last regular and the first singular solutions thus obtained. As in the studies of Sychev (1987) and Lam (1988) the marginal singularity is expected to occur at the first appearance of an isolated zero in the minimum u_{min} of the streamwise velocity across the layer, regarded as a function of x and of the parameter α. In computations it soon became clear, however, that the grid refinement required for maintaining the accuracy of the solution imposes strong limitations on the computational time. Also the marginal moving-wall singularity turned out to be much more sensitive to the grid and the parameter variations than its fixed-wall counterpart, because even with the α-step of order $10^{-3} - 10^{-4}$ the solutions obtained were either strongly singular or still too remote from separation, judging from the rate of approach of u_{min} to its zero limit. As an illustration, the dashed lines in figure 2(*a*) refer to our computation nearest to breakdown of the regular solution of the finite-difference equations with fixed grid parameters (the same as for the solid curves). One can notice here remarkably regular behaviour of the flow functions upstream of the incipient singularity with, however,

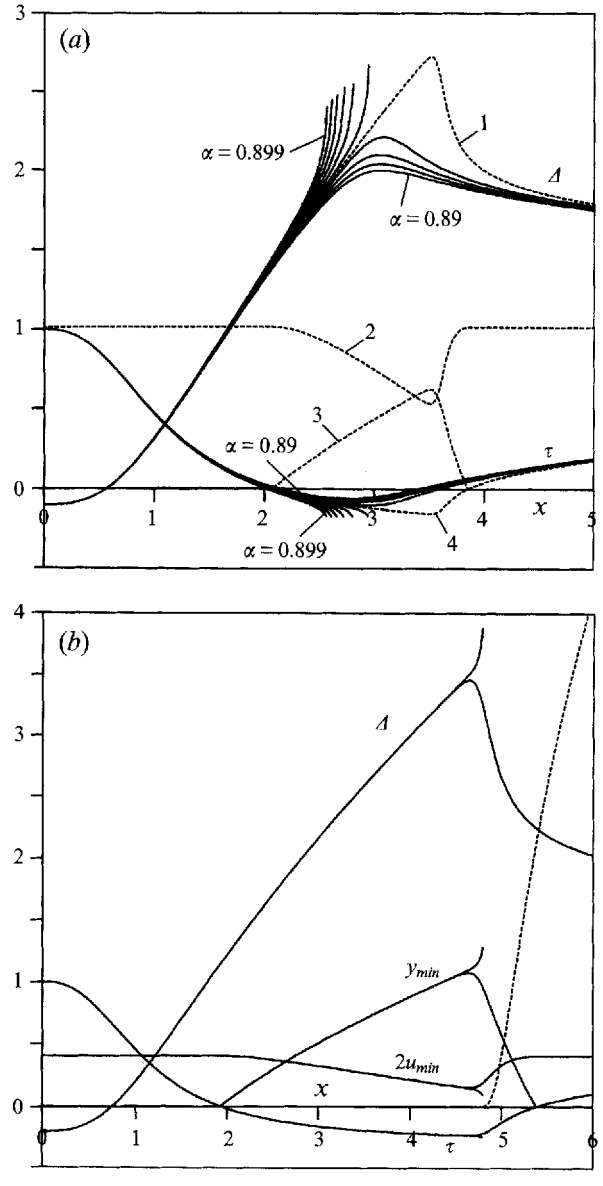

FIGURE 2. (*a*) The incipient singularity on the moving wall from solution of (2.1)–(2.5) with $\delta = 0.1$. The solid lines for the displacement thickness Δ and for the wall shear τ, *vs.* x, are drawn with the step $\Delta\alpha = 0.001$. The dashed lines 1–4 refer to the regular solution close to the breakdown obtained for $\alpha = 0.89343538$: $1, \Delta$; $2, 10u_{min}$; 3, the normal coordinate of the minimum velocity y_{min}; $4, \tau$. (*b*) The neighbouring regular and the first singular solutions of (2.1)–(2.5) with the slip increased to $\delta = 0.2$. The regular solution has $\alpha = 1.01448494$, $\Delta\alpha$ between the lines is 5×10^{-8}. The dashes show the function $(\Delta - \Delta_s)^4$ plotted for the comparison with the local solution (3.13).

stronger gradients immediately downstream. The streamwise velocity reaches its minimum, $u_{min} = 0.05$ or so, close to the maximum in the displacement thickness. The positioning of the minimum wall shear at approximately the same station may seem puzzling, but the explanation lies in the small value of the wall-slip velocity chosen and hence a relatively large ratio of u_{min} to the wall velocity. An analysis in § 4 deals

specifically with a complicated structure of the breakdown on a slowly moving wall which our computations are hardly capable of capturing in full detail.

With the slip velocity increased to $\delta = 0.2$ the location of marginal separation is shifted further downstream, $x_s = 4.6562$, and the maximum in the displacement thickness distribution becomes somewhat higher, $\Delta(x_s) = 3.4494$; see figure 2(*b*). In all other respects the pattern of the flow development repeats the previous case. Altogether, the computations in this section suggest the origin of separation at the regular *MRS* point first with, however, a slow approach to the limit solution. The dashed-line functions in figure 2(*a*), for example, require the corresponding value of $\alpha = 0.893435\ldots$ to be specified with an accuracy less than 10^{-7} but, of course, much larger approximation errors invalidate the last digits in this estimate for α_c.

3. Local analysis of the incipient singularity

The theory below aims to derive properties of the marginal boundary layer from local consideration in a small neighbourhood of the *MRS* point. First, we postulate a regular main flow upstream of the *MRS* point and examine possible continuations of the solution downstream. The second issue to be considered here concerns the behaviour of a slightly perturbed basic flow.

Let $\psi = \psi_0(x, y)$ denote a solution of (2.1) with a regular approach to the *MRS* point; the spatial coordinates of the latter are x_s, y_s. In the computations of the previous section this corresponds to the critical amplitude $\alpha = \alpha_c$ and hence to the specific pressure distribution, $p(x, \alpha_c) = p_0(x)$ say. At small distances upstream the streamfunction ψ_0 expands in a power series

$$\psi_0 = \psi_{00}(y) + (x_s - x)\,\psi_{01}(y) + O\left((x - x_s)^2\right), \tag{3.1}$$

where

$$\psi_{00} = a_{00} + \tfrac{1}{6}a_{03}(y - y_s)^3 + \ldots, \quad \psi_{01} = a_{10} + a_{11}(y - y_s) + \ldots \tag{3.2}$$

as $y \to y_s$, with constant coefficients a_{ij}. The constants a_{03}, a_{11} are assumed to be positive, the former on account of the adverse pressure gradient at $x = x_s$, $a_{03} = p_0'(x_s)$, and the latter from the requirement of the lack of reversed flow in the associated velocity profile

$$u_0 = \partial\psi_0/\partial y = \tfrac{1}{2}a_{03}(y - y_s)^2 + \ldots + a_{11}(x_s - x) + \ldots \tag{3.3}$$

at $x < x_s$. Also the *MRS* conditions of zero velocity and vorticity eliminate the linear and the quadratic terms in the expansion (3.2) for ψ_{00}. The streamfunction at $x < x_s$ can be extended analytically into the domain $x > x_s$, leading thereby to an entirely regular solution with flow reversal in the middle part of the boundary layer. Our computations in §2 suggest the possibility of a second solution with forward-flow velocity profiles and a singularity at $x_s + 0$.

The structure of this singular solution relies on a passive, effectively inviscid flow in the main part of the boundary layer, with the streamfunction given as

$$\psi_0 = \psi_{00}(y) + (x - x_s)^{1/4}\, c\psi_{00}'(y) + O\left((x - x_s)^{1/2}\right), \tag{3.4}$$

where the 'displacement' constant c must be zero in the interval $0 \leqslant y < y_s$, on account of the no-penetration condition at the wall. The value of c in the upper region $y > y_c$ follows from the solution for the intermediate nonlinear viscous layer

in the vicinity of the *MRS* point where

$$\psi_0 = a_{00} + (x - x_s)^{3/4} f(\eta) + \ldots, \quad \eta = (y - y_s)(x - x_s)^{-1/4} \tag{3.5}$$

and $\eta = O(1)$ as $x - x_s \to 0$. Substitution of (3.5) into (2.1) yields the equation

$$f''' + \tfrac{3}{4} f f'' - \tfrac{1}{2}(f')^2 = a_{03} \tag{3.6}$$

for the function $f(\eta)$, with the boundary conditions

$$f = \tfrac{1}{6} a_{03}(\eta + c)^3 + o(1) \quad \text{as} \quad \eta \to +\infty, \tag{3.7}$$

$$f = \tfrac{1}{6} a_{03}\eta^3 + o(1) \quad \text{as} \quad \eta \to -\infty, \tag{3.8}$$

from matching with the solution (3.4) above and below the inner layer. The change of variables

$$\eta = a_{03}^{-1/4}\left(z - \tfrac{1}{2} c a_{03}^{\ 1/4}\right), \quad f = a_{03}^{\ 1/4}\varphi, \quad \bar{c} = \tfrac{1}{2} c a_{03}^{\ 1/4} \tag{3.9}$$

reduces (3.6)–(3.8) to the form

$$\varphi''' + \tfrac{3}{4}\varphi\varphi'' - \tfrac{1}{2}(\varphi')^2 = 1; \quad \varphi = \tfrac{1}{6}(z \pm \bar{c})^3 + o(1) \quad \text{as} \quad z \to \pm\infty, \tag{3.10}$$

which also implies the evenness of the function $\varphi'(z)$. Because of the last property the solution domain can be reduced to $z \geqslant 0$.

The problem (3.10) was solved with two different numerical methods. One of them was based on a straightforward iterative solution of the equation for a given $\bar{c}$ in the interval $0 \leqslant z \leqslant z_{max}$ with the end-point constraints $\varphi(0) = 0$, $\varphi(z_{max}) = \frac{1}{6} z_{max}^3 + \frac{1}{2}\bar{c} z_{max}^2$, $\varphi'(z_{max}) = \frac{1}{2} z_{max} + \bar{c} z_{max}$, where $z_{max} = 10$ typically, and with the grid step $\Delta z = 0.002$. Appropriate values of $\bar{c}$ were chosen subsequently from the condition $\varphi''(0) = 0$. In the other method a *NAG* subroutine was used. Both sets of calculations indicate the existence of only two admissible solutions, illustrated in figure 3. One solution is simply $\varphi = \frac{1}{6} z^3$, $\bar{c} = 0$, as in the incoming flow; the zero value of $\bar{c}$ indicates the vanishing singular term in (3.4). The second solution has non-zero streamwise velocity $\varphi' > 0$ for all z with $\varphi'(0) = 1.6236$, and $\bar{c} = 1.2956$. In the course of preparation of the manuscript Dr V. B. Zametaev (private communication) has kindly informed us that the non-uniqueness in the formulation (3.10) has been known to him since his study of marginal separation at the trailing edge of a flat plate in 1991–1992 (unpublished results). The same problem was also studied in 1989 by Dr J. W. Elliott in connection with unsteady trailing-edge separation, whose paper currently in preparation confirms our numerical results.

Two features of the second solution should be mentioned here for qualitative comparison with computations in § 2. The minimum velocity has strongly asymmetric behaviour in the vicinity of the *MRS* point:

$$u_{min}(x) = a_{11}(x_s - x) + \ldots \quad \text{if} \quad x < x_s, \tag{3.11}$$

$$u_{min}(x) = a_{03}^{1/2}\varphi'(0)(x - x_s)^{1/2} + \ldots \quad \text{if} \quad x > x_s, \tag{3.12}$$

according to (3.3) and (3.5), (3.9). Also the displacement thickness, which was assumed to be regular at $x < x_s$, contains an algebraic singularity

$$\Delta(x) = \Delta(x_s) - 2\bar{c} a_{03}^{-1/4}(x - x_s)^{1/4} + \ldots, \quad \text{as} \quad x \to x_s + 0, \tag{3.13}$$

downstream from the *MRS* point, as follows readily from the general relation

$$\frac{\mathrm{d}\Delta}{\mathrm{d}x} = -\left(\frac{\partial\psi}{\partial x} \Big/ \frac{\partial\psi}{\partial y}\right)_{y\to\infty}. \tag{3.14}$$

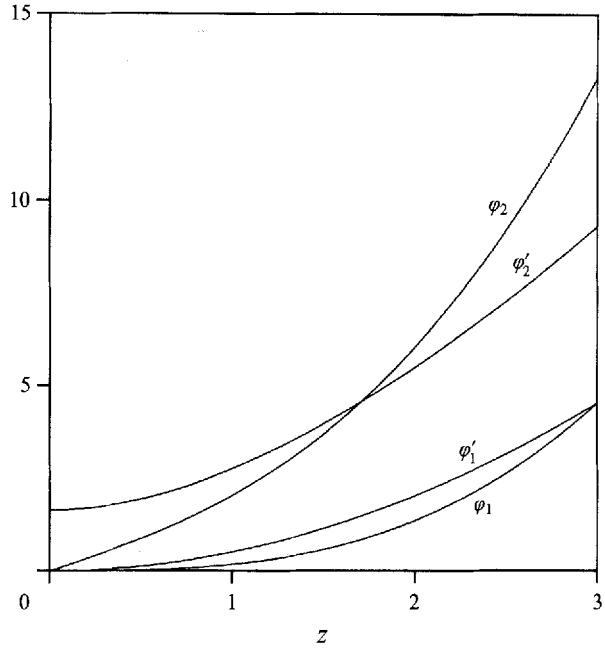

FIGURE 3. The streamfunction φ and the velocity φ' *vs.* z for the two solutions of (3.10); $\varphi_1 = \frac{1}{6}z^3$ is the unperturbed flow with $\bar{c} = 0$; φ_2 corresponds to the singular wake downstream of the *MRS* point.

In agreement with (3.13), the dashed line in figure 2(*b*) drawn for the computed function $(\Delta - \Delta(x_s))^4$ at $x \geqslant x_s$ has a clearly discernible portion of linear growth downstream of the incipient separation.

Further analysis can be made here in order to substantiate the appearance of incipient separation in the second, singular rather than in the regular form. We address now the changes in the main flow with the streamfunction $\psi_0(x, y)$ perturbed by small variations in the pressure distribution. Suppose that the pressure gradient contains a parameter α as, for example, in § 2, and that the specific value $\alpha_c$provides the basic-flow solution ψ_0. Then, with $\Delta\alpha = \alpha - \alpha_c$ small, the flow functions expand as

$$p' = p_0'(x) + \Delta\alpha p_1'(x) + O\left((\Delta\alpha)^2\right), \tag{3.15}$$

$$\psi = \psi_0(x, y) + \Delta\alpha\psi_1(x, y) + O\left((\Delta\alpha)^2\right), \tag{3.16}$$

where the perturbation term ψ_1 is governed by

$$\frac{\partial}{\partial x}\left(\frac{\partial\psi_0}{\partial y}\frac{\partial\psi_1}{\partial y}\right) - \frac{\partial\psi_0}{\partial x}\frac{\partial^2\psi_1}{\partial y^2} - \frac{\partial\psi_1}{\partial x}\frac{\partial^2\psi_0}{\partial y^2} + p_1'(x) = \frac{\partial^3\psi_1}{\partial y^3}, \tag{3.17}$$

with appropriate initial and boundary conditions.

The balance between the convective and viscous terms in (3.17), in conjunction with the vanishing main-flow velocity (3.1), (3.2), suggest an unusually strong singular behaviour of the perturbation

$$\psi_1 = \exp\left[\mu(x_s - x)^{-1} + O\left(\ln|x_s - x|\right)\right] F(\eta_1) + \ldots, \tag{3.18}$$

near the *MRS* point in the viscous layer $\eta_1 = (y - y_s)(x_s - x)^{-1/2} = O(1)$, where, on

substituting into (3.17), $F(\eta_1)$ satisfies the equation

$$F''' = \mu a_{03}\left[\left(\tfrac{1}{2}\eta_1^2 + a_{11}a_{03}^{-1}\right)F' - \eta_1 F\right]. \tag{3.19}$$

The boundary conditions

$$F = O\left(\eta_1^2\right) \quad \text{as} \quad \eta_1 \to +\infty; \quad F \to 0 \quad \text{as} \quad \eta \to -\infty, \tag{3.20}$$

follow from an analysis of the flow in the main part of the boundary layer, similar to (3.7). The required solution of (3.19), (3.20) must have the real part of μ positive and was given, in different notation, in Cowley *et al.* (1985). In particular,

$$\mu = \tfrac{1}{2}a_{03}\,a_{11}^{-2}, \tag{3.21}$$

and hence small changes in the flow conditions produce an exponentially strong local response in the perturbed flow field closer to the *MRS* point. Perhaps this explains the stringent requirements on the grid/parameter refinement encountered in our marching computations in §2.

The fast-growing perturbation term invalidates the expansion (3.16) at a small distance from x_s. The disturbance first becomes nonlinear in a viscous domain centred around y_s, where the leading terms in the streamfunction expansion are

$$\psi = a_{00} + \varepsilon^{1/2}a_{10} + \varepsilon^{3/4}a_{03}^{-1/2}a_{11}^{3/2}\overline{\psi}(\overline{x},\overline{y}) + \ldots. \tag{3.22}$$

Here the local variables $\overline{x},\overline{y}$ are introduced by

$$x = x_s - \varepsilon^{1/2} + \varepsilon a_{11}^2 a_{03}^{-1}\,\overline{x}, \quad y = y_s + \varepsilon^{1/4}\left(a_{11}/a_{03}\right)^{1/2}\overline{y}, \tag{3.23}$$

and ε is a small parameter such that

$$\Delta\alpha = \varepsilon^{3/4}\exp\left(-\mu\varepsilon^{-1/2}\right) \quad \text{or} \quad \varepsilon = \mu^2\left(\ln\frac{1}{\Delta\alpha}\right)^{-2} + \ldots. \tag{3.24}$$

The main nonlinear term in (3.22) is governed by the initial- and boundary-value formulation

$$\frac{\partial\overline{\psi}}{\partial\overline{y}}\frac{\partial^2\overline{\psi}}{\partial\overline{x}\partial\overline{y}} - \frac{\partial\overline{\psi}}{\partial\overline{x}}\frac{\partial^2\overline{\psi}}{\partial\overline{y}^2} + 1 = \frac{\partial^3\overline{\psi}}{\partial\overline{y}^3}, \tag{3.25}$$

$$\overline{\psi} = \tfrac{1}{6}\overline{y}^3 + \overline{y} + C\mathrm{e}^{\overline{x}/2}F\left(a_{11}^{1/2}a_{03}^{-1/2}\overline{y}\right) + o\left(\mathrm{e}^{\overline{x}/2}\right) \quad \text{as} \quad \overline{x} \to -\infty, \tag{3.26}$$

$$\overline{\psi} = \tfrac{1}{6}(\overline{y} - \overline{\Delta}(\overline{x}))^3 + \overline{y} - \overline{\Delta}(\overline{x}) + o(1) \quad \text{as} \quad \overline{y} \to +\infty, \tag{3.27}$$

$$\overline{\psi} = \tfrac{1}{6}\overline{y}^3 + \overline{y} + o(1) \quad \text{as} \quad \overline{y} \to -\infty. \tag{3.28}$$

As before, here the displacement function $\overline{\Delta}$ is present in the outer-edge condition (3.27) above the inner layer, but not in (3.28), cf. (3.8), (3.20). An additional shift in the origin $\overline{x} \to \overline{x}+\text{const}$ allows us to choose $C = 0, 1$, or -1, in the initial condition (3.26), and, consequently, the problem has three different solutions. One solution with $C = 0$ simply repeats the unperturbed flow: $\overline{\psi} = \overline{y} + \overline{y}^3/6$, $\overline{\Delta} = 0$. Two other solutions were obtained numerically with the method described in §2, except the domain of integration is now $\overline{x} \geqslant 0$, $|\overline{y}| \leqslant \overline{y}_{max}$ with the typical grid parameters $\overline{y}_{max} = 3, \Delta\overline{x} = 0.01, \Delta\overline{y} = 0.0015$. In computations the initial condition was replaced by

$$\overline{\psi} = \tfrac{1}{6}\overline{y}^3 + \overline{y} + C\overline{y}^2\mathrm{e}^{\overline{y}}\left(1 + \mathrm{e}^{\overline{y}}\right)^{-1} \quad \text{at} \quad \overline{x} = 0, \tag{3.29}$$

where $C = -10^{-3}$ and $+10^{-3}$ for the two cases illustrated in figures 4 and 5

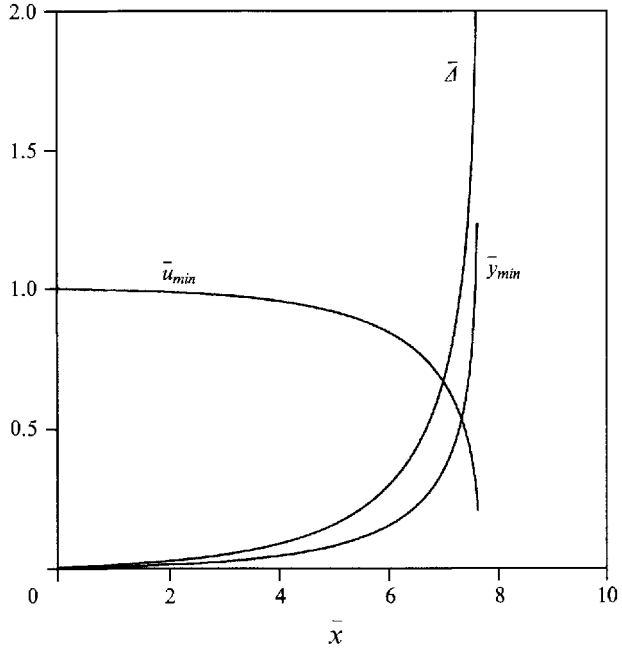

FIGURE 4. The displacement thickness $\bar{\Delta}$, the minimum velocity across the layer $\bar{u}_{min} = min\{\partial\bar{\psi}/\partial\bar{y}\}$ and the normal coordinate of the velocity minimum $\bar{y}_{min}$, *vs.* $\bar{x}$, for the singular decelerating solution of (3.25), (3.27)–(3.29) with $C = -10^{-3}$.

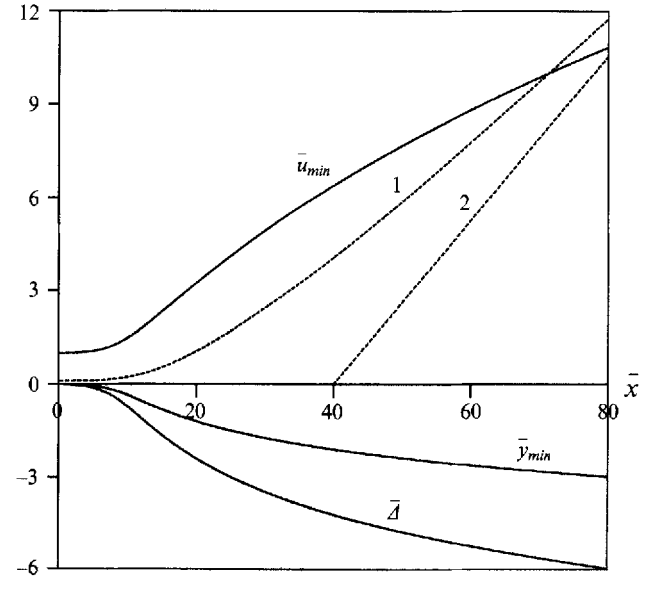

FIGURE 5. The flow functions $\bar{\Delta}$, $\bar{u}_{min}$, $\bar{y}_{min}$ *vs.* $\bar{x}$, as in figure 4 but for the regular accelerating solution of (3.25), (3.27)–(3.29) with $C = 10^{-3}$. The dashed line 1 drawn for the function $\frac{1}{10}\bar{u}^2_{min}$ and the straight line 2 given by $\bar{y} = 0.264(\bar{x} - 40)$ have equal slopes at large $\bar{x}$, in agreement with (3.5), (3.12).

respectively. Of course, more sophisticated techniques can be used in order to incorporate the specific initial condition (3.26); however the overall trends in the nonlinear flow development are hardly affected by our simplified choice. The reason for this lies in the nature of the exponential branching in the far-field asymptote. Unlike the conventional boundary-value problem for parabolic-type equations with the initial conditions specified at a finite x-section (at $x = 0$, for example), the initial velocity profile $\bar{u} = \partial\bar{\psi}/\partial\bar{y} = \bar{y}^2/2 + 1$ in (3.26) is given as $\bar{x} \to -\infty$. The steady two-dimensional boundary-layer flow with the parabolic velocity profile is known to be unstable, in a sense, to stationary disturbances (cf. Timoshin 1995 and the next section) and the joint influence of the two factors – the unbounded $\bar{x}$-domain and the instability – means that the exponentially small term must be retained in (3.26) in order to ensure the uniqueness of the solution. In the derivation above the eigenfunction was triggered by a distributed pressure variation (3.15) but, physically, any other source of disturbances, such as a local pressure variation, changes in the outer-edge or wall conditions, or even an artificial disturbance in the streamfunction distribution at a chosen x-station, must have a similar effect. Indeed, in some of our test computations the initial condition was taken in the form (3.29) with $C = 0$, but the pressure gradient in (3.25) was perturbed in a localized $\bar{x}$-interval by an amount of order 10^{-4}. This turned out to be sufficient to alter the solution nonlinearly further downstream, with the typical outcome in one of the two forms shown in figures 4 and 5; see also the next section. An additional small deceleration of the flow provokes the ultimate finite-distance termination of the solution with the Sychev (1980), Elliott *et al.* (1983) singularity, figure 4. By contrast, the slightly accelerated solution in figure 5 remains regular and evolves towards the self-similar limit (3.5) when $\bar{x} \to +\infty$ as follows from the behaviour of the computed function $\frac{1}{10}u_{min}^2(\bar{x})$, the dashed line in figure 5, showing the same finite slope at large $\bar{x}$ as the straight line 2 given by $\bar{y} = 0.264\ (\bar{x} - 40)$, in agreement with (3.12) with $a_{01} = 1, \varphi'(0) = 1.6236$. Small parametric deviations from the precisely regular approach to the *MRS* point inevitably switch the flow over to either strongly singular breakdown somewhat ahead of the *MRS* section, or to the entirely regular accelerating flow, in favourable agreement with the computational features in § 2.

4. Marginal separation on a slowly moving wall

In a two-parameter problem of the kind considered in § 2 the marginal solutions form a one-parameter family, so that, for example, the critical pressure amplitude α_c appears to be a function of the slip velocity δ, cf. figures 1 and 2(a, b). In general, further computations are required in order to establish the behaviour of the function $\alpha_c(\delta)$ in the entire δ-range, although some analysis is possible for small values of δ as we will show in this section where, starting with the well-known local structure of the fixed-wall flow, we derive all essential features of the moving-wall marginal singularity.

Here we suppose that the pressure gradient in (2.1), as well as the initial and the outer-edge conditions, are regular functions of α, whereas the wall condition in the form (2.2) contains the parameter δ only. The fixed-wall solution with the marginal singularity at $x = x_0$ is denoted as $\Psi_0(x, y)$, the corresponding pressure function is $p = P_0(x)$, and the value of the parameter is $\alpha_0\ (= \alpha_c(0))$. In the vicinity of x_0 we have $P_0'(x) = p_{00} + O(x - x_0)$ with a constant $p_{00} > 0$, and then the streamfunction

in the near-wall part of the flow expands as

$$\Psi_0 = \tfrac{1}{6}p_{00}y^3 + \tfrac{1}{2}a_0|x-x_0|y^2 + \ldots \quad \text{as} \quad y \to 0, |x-x_0| \to 0, \tag{4.1}$$

with a positive constant a_0; see Ruban (1981, 1982*a*) and Stewartson *et al.* (1982).

Consider alterations in the main flow (4.1) caused by the simultaneous effects of a small slip velocity $\delta \ll 1$ and variations in the external forcing. On setting $\Delta\alpha = \alpha - \alpha_0$, $|\Delta\alpha| \ll 1$, the imposed pressure gradient expands as

$$p' = P_0'(x) + \Delta\alpha P_1'(x) + O\left((\Delta\alpha)^2\right), \tag{4.2}$$

with similar expressions for the initial and the outer-edge boundary conditions, if necessary. At a finite distance upstream of the singular point the solution of (2.1), (2.2), (4.2) expands in the form

$$\psi = \Psi_0(x,y) + \delta\Psi_1(x,y) + \Delta\alpha\Psi_2(x,y) + \ldots, \tag{4.3}$$

with the linear perturbation terms $\Psi_i, i = 1,2$, satisfying

$$\frac{\partial}{\partial x}\left(\frac{\partial\Psi_0}{\partial y}\frac{\partial\Psi_i}{\partial y}\right) - \frac{\partial\Psi_0}{\partial x}\frac{\partial^2\Psi_i}{\partial y} - \frac{\partial\Psi_i}{\partial x}\frac{\partial^2\Psi_0}{\partial y^2} + \delta_{i2}P_1' = \frac{\partial^3\Psi_i}{\partial y^3}, \tag{4.4}$$

and the wall conditions

$$\Psi_i = 0, \frac{\partial\Psi_i}{\partial y} = \delta_{i1}u_w(x) \quad \text{at} \quad y = 0. \tag{4.5}$$

Here δ_{ij} is the Kronecker delta.

Solutions of the linear equations (4.4) develop algebraic singularities as $x \to x_0 - 0$. With regard to the $\Delta\alpha$-induced term Ψ_2, this was established in Ruban (1981, 1982*a*) and Stewartson *et al.* (1982). In particular,

$$\Psi_2 = a_2(x_0-x)^{-1}y^2 + \ldots, \quad x \to x_0 - 0, \; y \to 0 \tag{4.6}$$

represents the leading term in the perturbed streamfunction in the near-wall domain with the typical thickness $y = O\left((x_0-x)^{1/4}\right)$. The constant a_2 here is determined by global solution of the problem. A complementary solution in the main part of the boundary layer, $\Psi_2 = 2a_2p_{00}^{-1}(x_0-x)^{-1}\partial\Psi_0(x_0,y)/\partial y + \ldots$, follows then from locally-inviscid balancing in (4.4) and the match with (4.6). In this section, owing to the dominant role of the near-wall regions in the formation of singularities, we can often disregard the passive upper part of the boundary layer.

A singular expression similar to (4.6) also holds for the slip-induced component Ψ_1. For a particular solution

$$\Psi_1 = u_w(x)\frac{\partial\Psi_0(x,y)}{\partial y}\Big/\frac{\partial^2\Psi_0(x,0)}{\partial y^2} \tag{4.7}$$

satisfies equation (4.4) and the trivial outer-edge condition and yields the local behaviour $\Psi_1 = u_w(x_0)p_{00}(2a_0)^{-1}y^2(x_0-x)^{-1} + \ldots$, cf. Timoshin (1988), whereas the initial condition, which we do not discuss here explicitly, can be violated. The required correction term, being governed by the homogeneous equation with trivial conditions at $y = 0$, can alter the coefficient, but not the type of singularity in the general case. Hence

$$\Psi_1 = a_1(x_0-x)^{-1}y^2 + wy + \ldots \quad \text{as} \quad x \to x_0 - 0, \; y \to 0, \tag{4.8}$$

without loss of the generality, where a_1 is a constant, $w = u_w(x_0)$ and we retain the higher-order term associated with the motion of the wall.

The outer solution (4.3), (4.6), (4.8) ceases to be valid in a small neighbourhood of x_0 in the inner region with the spatial scales $x - x_0 = O(\delta^{1/2})$, $y = O(\delta^{1/8})$ if we assume, to start with, that $\Delta\alpha = O(\delta)$. A technique similar to that in Ruban (1981, 1982*a*) and Stewartson *et al.* (1982) yields then

$$\psi = \tfrac{1}{6}p_{00}y^3 + \tfrac{1}{2}y^2\left(a_0^2(x-x_0)^2 + 4a_0(\Delta\alpha a_2 + \delta a_1)\right)^{1/2} + \ldots \tag{4.9}$$

for the streamfunction in the inner domain. The inner solution is regular (singular) when the combination $\kappa = \Delta\alpha a_2 + \delta a_1$ is positive (negative) and hence the leading-order effect of a small slip velocity turns out to be fairly straightforward: the critical value α_c is shifted from α_0 by an amount of order δ, whereas the form and the location of the marginal separation remain unaltered. It is important to note that κ is equal to the total coefficient of the algebraic singularity in the outer solution (4.3), to leading order.

Closer to the new threshold value $\alpha_c = \alpha_0 - \delta a_1/a_2$, however, the flow in the inner region becomes affected by the wall velocity through a mechanism similar to that in Elliott *et al.* (1983). Assuming, for example, that the slip velocity δ is fixed and α varies we define

$$\alpha = \alpha_0 - \delta a_1 a_2^{-1} + \delta^{8/5}\alpha_1, \quad \alpha_1 = O(1), \tag{4.10}$$

and seek a solution of (2.1) in the form

$$\psi = \delta^{3/5}\tfrac{1}{6}p_{00}Y^3 + \delta^{6/5}\left(\tfrac{1}{2}Y^2A(X) + wY\right) + \ldots + \delta^{9/5}\tilde{\psi} + \ldots \tag{4.11}$$

in the region $Y = y\delta^{-1/5} = O(1)$, $X = (x - x_0)\delta^{-4/5} = O(1)$.

The equation for the main-order wall shear $A(X)$ is derived from the analysis of the boundary-value problem

$$\frac{\partial^3\tilde{\psi}}{\partial Y^3} - p_{00}\left(\frac{1}{2}Y^2\frac{\partial^2\tilde{\psi}}{\partial X\partial Y} - Y\frac{\partial\tilde{\psi}}{\partial X}\right) = \tfrac{1}{2}Y^2AA' + wYA', \tag{4.12}$$

$$\tilde{\psi} = \frac{\partial\tilde{\psi}}{\partial Y} = 0 \quad \text{at} \quad Y = 0; \quad \frac{\partial^3\tilde{\psi}}{\partial Y^3} \to 0 \quad \text{as} \quad Y \to \infty \tag{4.13}$$

for a contribution to the higher-order term $\tilde{\psi}$ in (4.11) non-polynomial in X and Y. The usual solvability requirement yields the integro-differential equation

$$\overline{A}^2 - \overline{X}^2 + \overline{\gamma} = -s\int_{-\infty}^{\overline{X}}\left(\overline{A}'(t) + 1\right)\frac{\mathrm{d}t}{\left(\overline{X} - t\right)^{1/4}}, \tag{4.14}$$

with the initial condition

$$\overline{A} = -\overline{X} + \overline{\gamma}\left(2\overline{X}\right)^{-1} + \ldots \quad \text{as} \quad \overline{X} \to -\infty, \tag{4.15}$$

cf. Ruban (1982*b*) and Smith (1982*b*). Here

$$\overline{X} = a_0^{4/5}|\gamma|^{-4/5}X, \quad \overline{A} = a_0^{-1/5}|\gamma|^{-4/5}A, \quad s = \operatorname{sign}(w), \tag{4.16}$$

$$\gamma = 4w(2p_{00})^{1/4}\pi^{-4}\Gamma\left(\tfrac{3}{4}\right), \quad \overline{\gamma} = -4a_0^{3/5}a_2\alpha_1|\gamma|^{-8/5}, \tag{4.17}$$

and $\Gamma(z)$ is the gamma-function.

The solutions of (4.14), (4.15) illustrated in figure 6 for the case of the downstream-moving wall, $s = 1$, were obtained numerically with a second-order-accurate method marching from $\overline{X} = -5$ with the typical step $\Delta\overline{X} = 0.005$. Owing to the lack of

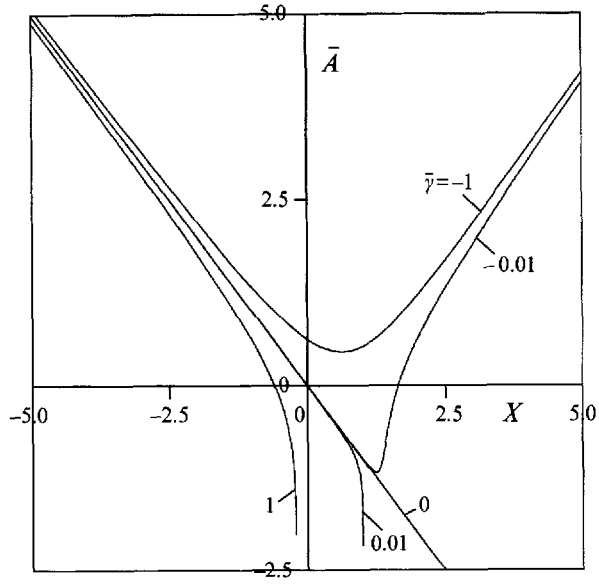

FIGURE 6. The scaled wall shear $\overline{A}$ *vs.* $\overline{X}$ from solution of (4.14) with $s = 1$ for various $\overline{\gamma}$.

the parameter $\overline{\gamma}$ indicated on the figure. The critical value is $\overline{\gamma} = 0$ $(\overline{A} = -\overline{x})$, for it divides the families of regular $(\overline{\gamma} < 0)$ and singular $(\overline{\gamma} > 0)$ solutions. The finite-distance termination of the solutions is accompanied by an unbounded decrease of the wall shear,

$$\overline{A} = -\frac{(\pi)^{1/2}}{4}\frac{\Gamma\left(\frac{3}{4}\right)}{\Gamma\left(\frac{5}{4}\right)}\left(\overline{X}_s - \overline{X}\right)^{-1/4} + \ldots, \tag{4.18}$$

with the position of the singularity $\overline{X}_s$ determined by the whole solution. The next stage in the development of this singularity invokes the fully nonlinear equation (2.1), but on a shorter x-scale, with the subsequent locally inviscid breakdown, see Elliott *et al.* (1983). The implication is that the entire parameter range $\overline{\gamma} > 0$ provides strongly singular terminations in the full problem.

In the near-marginal limit $\overline{\gamma} \to 0$ an expansion of the form

$$\overline{A} = -\overline{X} + \overline{\gamma}\overline{A}_1(\overline{x}) + O\left(\overline{\gamma}^2\right) \tag{4.19}$$

yields

$$\overline{A}_1 = -\frac{1}{2}\int_0^\infty \exp\left[-\tfrac{2}{5}\Gamma\left(\tfrac{3}{4}\right)t^{5/4} + t\overline{X}\right]\mathrm{d}t, \tag{4.20}$$

and hence

$$\overline{A}_1 = -\pi^{1/2}2^{5/2}\left[\Gamma\left(\tfrac{3}{4}\right)\right]^{-2}\overline{X}^{3/2}\exp\left[\tfrac{1}{5}\theta_0\overline{X}^5\right] + \ldots \quad \text{as} \quad \overline{X} \to +\infty, \tag{4.21}$$

where $\theta_0 = 16\left[\Gamma\left(\frac{3}{4}\right)\right]^{-4}$, cf. Brown & Stewartson (1983). This shows that small deviations from the linear function $\overline{A} = -\overline{X}$ restore the nonlinearity at a distance $L \gg 1$ from the origin, where

$$L = \left[-5\theta_0^{-1}\ln|\overline{\gamma}|\right]^{1/5} + \ldots \quad \text{as} \quad \overline{\gamma} \to 0. \tag{4.22}$$

The governing equation for the nonlinear readjustment region is obtained by making

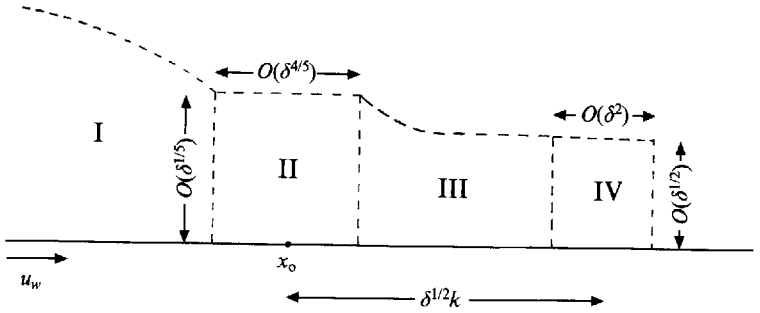

FIGURE 7. A sketch illustrating the asymptotic splitting of the near-wall part of the marginally separated boundary layer on a slowly moving surface; x_0 marks the position of the fixed-wall marginal separation and, at leading order, the point of zero wall shear in the moving-wall problem: I, viscous layer of thickness $(x_0 - x)^{1/4}$ upstream of x_0; II, the region governed by (4.14); III, the region of exponential amplification of the disturbance (4.43); IV, the central nonlinear domain with the controlling equations (4.28)–(4.32).

the substitution

$$\overline{X} = L + L^{-4}z, \quad \overline{A} = LB(z) \tag{4.23}$$

into (4.14) with $s = 1$. The result is

$$B^2 - 1 = -\int_{-\infty}^{z} B'(s)\,\frac{\mathrm{d}s}{(z-s)^{1/4}}, \tag{4.24}$$

which should be solved subject to

$$B = -1 - \operatorname{sign}(\overline{\gamma})\exp(\theta_0 z) + \ldots \quad \text{as} \quad z \to -\infty \tag{4.25}$$

on account of matching with (4.19), (4.21). The formulation for the readjustment zone was studied earlier in Smith & Elliott (1985) in the context of unsteady boundary-layer dynamics. They show that there exist three solutions of the problem: the unperturbed flow with $B = -1$, $\operatorname{sign}(\overline{\gamma}) = 0$, the solution with a finite-distance singularity (4.18) when $\operatorname{sign}(\overline{\gamma}) = 1$, and the regular shock-layer solution for $\operatorname{sign}(\overline{\gamma}) = -1$ with the behaviour $B(z) \to 1$ far downstream. In the latter case, which gives the appropriate form of the subcritical flow in figure 6 as $\overline{\gamma} \to -0$, the approach to the far-downstream limit is algebraic and hence the representation (4.19) has to be replaced by $\overline{A} = \overline{X} + O(\overline{\gamma})$ in the domain $\overline{X} > L$.

Equation (4.14) was derived under the assumption that the variation of the parameter α in (4.10) is of order $\delta^{8/5}$ when $\delta \to 0$. Within this α-interval the marginal solution turns out to be specified by the condition $\overline{\gamma} = 0$ or, equivalently, $\alpha_1 = 0$. In other words, the near-marginal solutions can be extended further downstream if the coefficient of the algebraic singularity κ in the outer solution (4.3), (4.6), (4.8) is made smaller than $O(\delta^{8/5})$. In fact, it has to be exponentially small, as we shall show shortly.

When α_1 in (4.10) and $\overline{\gamma}$ in (4.14) become sufficiently small in absolute value the nonlinear readjustment zone (4.23) moves downstream until the controlling equation for this region acquires a fully nonlinear form. The sketch in figure 7 illustrates the asymptotic structure of the flow field for this new regime. The distance between the nonlinear zone IV, which will be playing the central part in the remainder of this section, and the position of the marginal fixed-wall singularity is $\delta^{1/2}k$, $k = O(1)$, whilst the streamwise extent of the nonlinear zone is much smaller, of order δ^2. The

solution here is sought in the form

$$\psi = \delta^{3/2} p_{00} \tilde{w}^3 \tilde{\psi}(\tilde{x}, \tilde{y}) + \ldots, \tag{4.26}$$

$$x = x_0 + \delta^{1/2} k + \delta^2 p_{00} \tilde{w}^4 \tilde{x}, \quad y = \delta^{1/2} \tilde{w} \tilde{y}, \tag{4.27}$$

where $\tilde{w} = w/(ka_0)$, $(\tilde{x}, \tilde{y}) = O(1)$. Substitution of (4.26), (4.27) into (2.1) yields the Prandtl equation

$$\frac{\partial \tilde{\psi}}{\partial \tilde{y}} \frac{\partial^2 \tilde{\psi}}{\partial \tilde{x} \partial \tilde{y}} - \frac{\partial \tilde{\psi}}{\partial \tilde{x}} \frac{\partial^2 \tilde{\psi}}{\partial \tilde{y}^2} + 1 = \frac{\partial^3 \tilde{\psi}}{\partial \tilde{y}^3}, \tag{4.28}$$

to leading order. The initial and boundary conditions are

$$\tilde{\psi} = 0, \quad \frac{\partial \tilde{\psi}}{\partial \tilde{y}} = b \quad \text{at} \quad \tilde{y} = 0, \tag{4.29}$$

$$\tilde{\psi} \to \tfrac{1}{6}\tilde{y}^3 - \tfrac{1}{2} b \tilde{y}^2 + b\tilde{y} \quad \text{as} \quad \tilde{x} \to -\infty, \tag{4.30}$$

$$\tilde{\psi} = \tfrac{1}{6}(\tilde{y} - \tilde{\Delta}(\tilde{x}) + b)^3 - \tfrac{1}{2} b(\tilde{y} - \tilde{\Delta}(\tilde{x}) + b)^2 + b(\tilde{y} - \tilde{\Delta}(\tilde{x}) + b) + o(1) \quad \text{as} \quad \tilde{y} \to \infty, \tag{4.31}$$

on account of (2.2), (4.11), (4.19). The parameter $b = k^2 a_0^2 p_{00}^{-1} w^{-1}$ marks the position of the nonlinear region in the flow field. Apart from the slip condition (4.29), the formulation (4.28)–(4.31) resembles closely the problem (3.25)–(3.28) from the previous section, and, following the scenario therein, the exact solution in the form $\tilde{\psi} = \frac{1}{6}\tilde{y}^3 - \frac{1}{2} b \tilde{y}^2 + b\tilde{y}$, $\tilde{\Delta} = b$, turns out to be non-unique owing to an exponential bifurcation at minus infinity. Setting

$$\tilde{\psi} = \tfrac{1}{6}\tilde{y}^3 - \tfrac{1}{2} b \tilde{y}^2 + b\tilde{y} + \tilde{c} \exp(\tilde{\mu}\tilde{x}) \tilde{f}(y) + \ldots \quad \text{as} \quad \tilde{x} \to -\infty, \tag{4.32}$$

$$\tilde{u}_0 = \tfrac{1}{2}\tilde{y}^2 - b\tilde{y} + b, \tag{4.33}$$

with constant $\tilde{c}, \tilde{\mu}$, we arrive at the eigenvalue problem

$$\tilde{f}''' = \tilde{\mu}\left(\tilde{u}_0 \tilde{f}' - \tilde{u}_0' \tilde{f}\right), \quad \tilde{f}(0) = \tilde{f}'(0) = \tilde{f}'''(\infty) = 0 \tag{4.34}$$

for the perturbed streamfunction $\tilde{f}(\tilde{y})$. Our concern is with the parameter range $0 < b < 2$, in which the in-flow velocity $\tilde{u}_0$ in (4.33) is strictly positive. As discussed in Timoshin (1995), the solution of (4.34) with $\tilde{\mu} > 0$ is unique, for a fixed b. The dependence $\tilde{\mu}(b)$ proves to be monotonic, with the limiting properties

$$\tilde{\mu} = 2\left[\Gamma\left(\tfrac{5}{4}\right)/\Gamma\left(\tfrac{3}{4}\right)\right]^4 + \ldots \quad \text{as} \quad b \to 0, \tag{4.35}$$

$$\tilde{\mu} = \tfrac{1}{2}(2-b)^{-2} + \ldots \quad \text{as} \quad b \to 2 - 0. \tag{4.36}$$

Next, the non-trivial eigenfunction in the far field suggests the existence of two perturbed solutions of the full nonlinear problem (4.28)–(4.31) with the initial condition in the form (4.32) and with $\tilde{c} = \pm 1$, on account of a shift transformation in $\tilde{x}$.

With the same argument as in § 3, we chose to compute the solution of (4.28)–(4.32) using the initial condition (4.30) applied at $\tilde{x} = 0$. In the two cases illustrated in figures 8 and 9 (the grids $\Delta\tilde{x} = 0.0005, \Delta\tilde{y} = 0.00125, \tilde{y}_{max} = 10$ and $\Delta\tilde{x} = 0.005, \Delta\tilde{y} = 0.005, \tilde{y}_{max} = 20$ respectively) the incoming flow (4.30) is perturbed by a small pressure disturbance

$$\mathrm{d}\tilde{p}/\mathrm{d}\tilde{x} = 1 + h_p \tilde{x}^2 (\tilde{x} - 2)^2, \tag{4.37}$$

which in the interval $0 \leqslant \tilde{x} \leqslant 2$ replaces the unit pressure gradient in the momentum equation. Further downstream the pressure gradient is maintained constant, $\mathrm{d}\tilde{p}/\mathrm{d}\tilde{x} =$

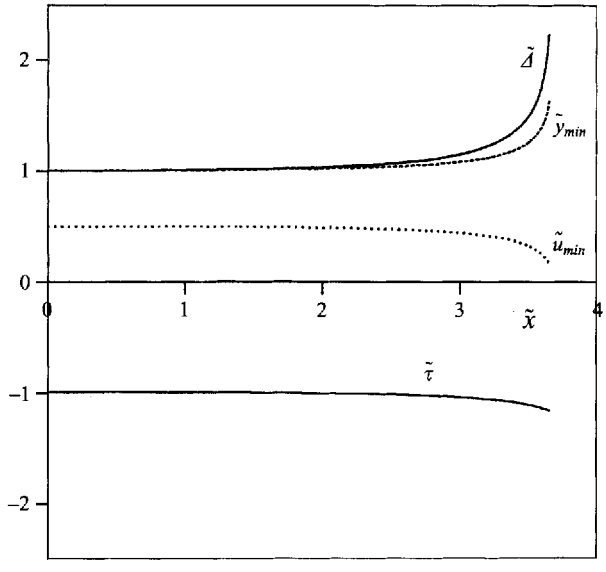

FIGURE 8. Singularity in the solution of (4.28)–(4.32), (4.37) with $b = 1$, $h_p = 0.001$: the wall shear $\tilde{\tau} = \partial^2\tilde{\psi}/\partial\tilde{y}^2\,(\tilde{y} = 0)$, the displacement thickness $\tilde{\Delta}$, the vertical coordinate $\tilde{y}_{min}$ of the minimum velocity, and the value of the velocity minimum $\tilde{u}_{min} = min\,\{\partial\tilde{\psi}/\partial\tilde{y}\}$, *vs.* the scaled coordinate $\tilde{x}$.

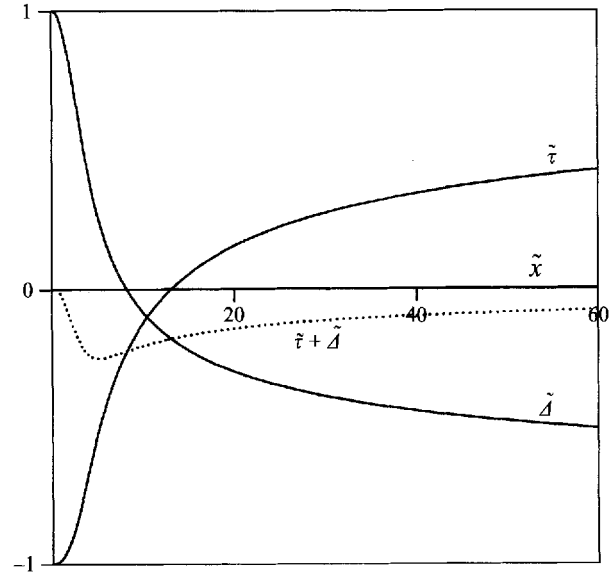

FIGURE 9. The regular solution of (4.28)–(4.32), (4.37) with $b = 1$, $h_p = -0.01$: the wall shear $\tilde{\tau}$, the displacement thickness $\tilde{\Delta}$, and the sum $\tilde{\tau} + \tilde{\Delta}$, *vs.* $\tilde{x}$.

1; nevertheless the flows with $h_p = 0.001$, $h_p = -0.01$ (figures 8 and 9 respectively) do not return to their original form. It was verified numerically that the entire range $h_p > 0$ provides solutions with strong singularities. In the limit $h_p \to 0$ the position of the finite-distance breakdown moves downstream, so that the observed deviation from the initial state (4.30) clearly becomes due to the pressure-induced eigenfunction (4.32) with $\tilde{c} < 0$ (provided that the normalization $\tilde{f}''(\infty) = 1$ is used). The opposite

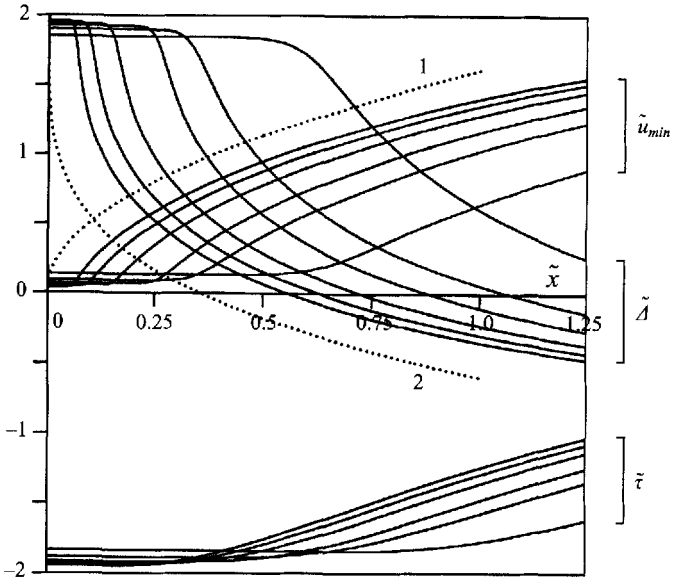

FIGURE 10. The regular solutions of (4.28)–(4.32), (4.39) for decreasing values of $2-b$. The solid lines show the minimum velocity $\tilde{u}_{min}$, the displacement thickness $\tilde{\Delta}$ and the wall shear $\tilde{\tau}$ vs $\tilde{x}$ for $b = 1.85, 1.9, 1.925, 1.94, 1.95, 1.96$ (the arrows indicate increasing b). For the comparison with (3.5), the dotted lines 1, 2 show the limiting forms $\tilde{u}_{min} = 1.6236\tilde{x}^{1/2}$, $\tilde{\Delta} = 2 - 2 \times 1.2956\tilde{x}^{1/4}$ respectively derived from (3.12), (3.13) with $\Delta(x_s) = 2$, $a_{03} = 1$ and with the values of $\varphi'(0)$, $\bar{c}$ given in the text.

sign in the pressure perturbation produces regular, accelerated-flow solutions with the asymptote

$$\tilde{\psi} = \tfrac{1}{6}\tilde{y}^3 + b_1\tilde{y}^2 + b\tilde{y} \quad \text{as} \quad \tilde{x} \to \infty \tag{4.38}$$

far downstream, where b_1 is a positive constant whose value depends on b and h_p. The comparison is made in figure 9 where the sum $\tilde{\tau} + \tilde{\Delta}$ is seen to have zero limit as $\tilde{x} \to \infty$.

Of especial interest for the main subject of this paper is the limiting form of the regular solutions of (4.28)–(4.32) as $b \to 2 - 0$. In computations for small positive values of $2-b$ the grid ($\Delta\tilde{x} = 0.00125, \Delta\tilde{y} = 0.0025, \tilde{y}_{max} = 5$) and the pressure gradient are kept constant whereas the source of disturbances was incorporated in the initial condition

$$\tilde{\psi} = \tfrac{1}{6}\tilde{y}^3 - \tfrac{1}{2}b\tilde{y}^2 + b\tilde{y} - 10^{-4}\tilde{y}^2, \tag{4.39}$$

imposed at $\tilde{x} = 0$; the last term in (4.39) is equivalent to a small increase in the wall velocity downstream of the origin. The sequence of solutions for progressively decreasing values of $2-b$ is shown in figure 10, where the trend towards the formation of a singular structure in the middle of the flow as $b \to 2 - 0$ is evident in the much delayed and relatively quiet development of the skin friction compared to the fast initial decrease in the displacement thickness correlated with the acceleration of the fluid particles in the middle part of the flow. In the limit $b = 2 - 0$ the solution of the problem (4.28)–(4.32) consists of the regular flow field upstream of a certain point which can be chosen as $\tilde{x} = 0$, with the singular start of the flow acceleration immediately downstream. Except for insignificant changes due to the scalings (4.26), (4.27), the ensuing inner structure with a viscous sublayer near the *MRS* point performs the same functions as the inner region in § 3.

In figure 7 the limit $b \to 2-0$ implies the shift of the nonlinear domain IV downstream closer to the point of flow reversal in the regular solution of the full boundary-layer equations. Thus the case of a small slip velocity gives extra credibility to the proposed marginal structure of § 3 with a regular flow field upstream of the *MRS* point.

Finally here we note that the flow structure in figure 7 holds only if, for a given slip δ, the variable pressure parameter α is specified with an extremely high accuracy. Indeed, in the upstream part of the flow (zone I) we require that the streamfunction and the parameter expand as

$$\psi = \sum_{n=0}^{\infty} \delta^n \psi_n(x,y) + \nu(\delta)\,\psi'(x,y), \quad \alpha = \sum_{n=0}^{\infty} \delta^n \alpha_n + \nu(\delta), \tag{4.40}$$

where $\nu(\delta)$ is assumed to be smaller than any integer power of δ and the constants α_n are chosen such that the corresponding terms ψ_n remain regular as $x \to x_0 - 0$. The term $\psi'(x,y)$ represents imperfections in the solution, so that

$$\psi' = a' y^2 (x_0 - x)^{-1} + \ldots \quad \text{as} \quad y \to 0,\ x \to x_0 - 0, \tag{4.41}$$

and a' is a constant, cf. (4.6), (4.8). The regular (power series) part of the streamfunction in (4.40) continues analytically across the x_0-section into zones II, III, whereas the singular term ψ' changes strongly on passing through the intermediate regions. First in zone II, where $x - x_0 = O\left(\delta^{4/5}\right)$, the algebraic singularity in (4.41) is smoothed out and then turned into a fast growing exponential function of the form

$$\psi' = C_{II}\,\delta^{-14/5} \exp\left[\tfrac{1}{5}\delta^{-4}\theta_0\, a_0^4\, \gamma^{-4}(x - x_0)^5\right] + \ldots \tag{4.42}$$

immediately downstream of zone II, cf. (4.21); here C_{II} is an insignificant order-one coefficient and other constants are as in (4.17), (4.21). Next, in zone III with the spatial variables $x - x_0 = \delta^{1/3} x_3$, $y = \delta^{1/2} y_3$, $(x_3, y_3) = O(1)$, the perturbation acquires the form

$$\psi' = \delta^{-41/20} \exp\left[\mu_3(x_3)\,\delta^{-3/2}\right] f_3(x_3, y_3) + \ldots, \tag{4.43}$$

where μ_3, f_3 follow directly from the solution of the problem (4.34) with

$$\frac{\mathrm{d}}{\mathrm{d}\tilde{y}};\ \tilde{f};\ \tilde{\mu};\tilde{u}_0 \tag{4.44}$$

replaced by

$$\frac{\mathrm{d}}{\mathrm{d}y_3};\ f_3;\ \frac{\mathrm{d}\mu_3}{\mathrm{d}x_3};\ \tfrac{1}{6}p_{00}y_3^3 - \tfrac{1}{2}a_0 x_3 y_3^2 + w y_3, \tag{4.45}$$

respectively. Note that in the eigenvalue problem so obtained the local streamwise coordinate x_3 appears as a parameter. Finally, the perturbed streamfunction (4.43) contributes nonlinearly to the regular part in (4.40) on approach to zone IV. Hence

$$\nu(\delta) = O\left(\delta^{71/20}\right) \exp\left[-\mu_3(\kappa)\,\delta^{-3/2}\right] \tag{4.46}$$

provides the order-of-magnitude estimate for admissible variations in α in (4.40).

5. Discussion

The main conclusion of this work is that marginal separation in the downstream-moving-wall boundary layer can occur under an adverse pressure gradient, and various parts of the analysis indicate that the flow breakdown studied here can

appear in a broad range of applications. The singular structure in §3 holds for a general boundary layer. The flow regime in §2 is best known in the theory of boundary layers over surface roughnesses; see e.g. Smith (1982*a*), Smith *et al.* (1981), Sychev *et al.* (1987) and Timoshin & Smith (1995). The statement of the problem in the previous section was made deliberately formal in order to emphasize the typical nature of the phenomenon, with, however, immediate applications to the leading-edge flow of Telionis & Werle (1973), for example. Nevertheless, and as a good starting point for a futher study, our analysis does not exclude other possibilities such as the breakdown in the rotating-cylinder problem. Computations in Nikolayev (1982) and Lam (1988) provide very strong evidence in favour of a zero pressure gradient at incipient separation. The structure proposed in the present paper with regular flow upstream of the *MRS* point cannot be transferred to the point of maximum pressure simply because the appropriate solution in the boundary layer does not exist; see Sychev (1987). It is possible, of course, that the breakdown on the rotating cylinder develops at a numerically small, but still finite, distance upstream of the pressure maximum. The complexity of the problem in general is also evident in the computations reported by Lam (1988) and S. J. Cowley (1994, private communication) for a model situation similar to that in §2, but with the pressure gradient changing sign from adverse to favourable at a finite distance from the starting section, which brings the flow conditions closer to the rotating-cylinder problem. Although the singularity in their case tends to appear near the point of zero pressure gradient, the gap between the position of the maximum in the displacement thickness and the alleged location of the singularity decreases too slowly to be conclusive. In any case, the existence of our and Sychev's candidates for the marginal singularity makes the problem quite different from its fixed-wall counterpart, where there seems to be no alternative to the solution described in Ruban (1981, 1982*a*) and Stewartson *et al.* (1982). Perhaps, a formulation of the type considered in §2, but with an x-periodic pressure and either zero or non-trivial (positive or negative) slip at the wall would be worth studying in this context, cf. Lam (1988).

Many studies on high-Reynolds-number separated flows support the view that flow regimes containing classical boundary layers should be regarded as physically sensible as long as the solution in the boundary layer remains regular, so that the marginal breakdown often gives the first indication of approaching global changes in the flow pattern. In a parameter-varying flow the next stage in the development of separation usually invokes an interaction between the boundary layer and the external potential flow. Negoda & Sychev (1987) consider effects of interaction in the flow with the inviscid marginal singularity; the equivalent of their theory in our case is a more difficult task, for it involves a necessarily numerical treatment of an interactive version of the fully nonlinear viscous formulation (3.25)–(3.28).

Extension of this work to time-varying and three-dimensional flows should also prove interesting. In the simplest self-similar regimes two-dimensional unsteady and three-dimensional steady boundary layers are governed by effectively two-dimensional strictly parabolic equations and admit, therefore, all essential features of planar steady flow, including the possibility of strong and marginal singularities; see e.g. Elliott *et al.* (1983) and Zametaev (1987). Effects of non-similarity, on the other hand, bring about the hyperbolic properties of the controlling equations and can alter the form and the entire meaning of the marginal separation, cf. Zametaev (1989), Cowley, Van Dommelen & Lam (1990).

The author is grateful to Professor S. N. Brown and Dr J. W. Elliott for numerous

suggestions on improvement of the manuscript, to Drs S. J. Cowley and S. T. Lam for sending their unpublished numerical results, to Professor F. T. Smith and Dr V. B. Zametaev for their interest and discussion, and to referees for their comments.

REFERENCES

BROWN, S. N. & STEWARTSON, K. 1983 On an integral equation of marginal separation. *SIAM J. Appl. Maths* **43**, 1119–1126.

CHANG, P. K. 1976 *Control of Flow Separation.* McGraw-Hill.

COWLEY, S. J., HOCKING, L. M. & TUTTY, O. R. 1985 The stability of solutions of the classical unsteady boundary-layer equation.*Phys. Fluids* **28**, 441–443.

COWLEY, S. J., VAN DOMMELEN, L. L. & LAM, S. T. 1990 On the use of lagrangian variables in descriptions of unsteady boundary-layer separation. *Phil. Trans. R. Soc. Lond.* A **333**, 343–378.

ELLIOTT, J. W., SMITH, F. T. & COWLEY, S. J. 1983 Breakdown of boundary layers: (i) on moving surfaces; (ii) in semi-similar unsteady flow; (iii) in fully unsteady flow. *Geophys. Astrophys. Fluid Dyn.* **25**, 77–138.

GOLDSTEIN, S. 1948 On laminar boundary-layer flow near a position of separation. *Q. J. Mech. Appl. Maths* **1**, 43–69.

LAM, S. T. 1988 On high-Reynolds-number laminar flows through a curved pipe, and past a rotating cylinder. PhD thesis, University of London.

NEGODA, V. V. & SYCHEV, V. V. 1987 Concerning boundary layer on a rapidly rotating cylinder. *Izv. Akad. Nauk. SSSR, Mekh. Zhidk. i Gaza* **5** , 36–45.

NIKOLAYEV, K. V. 1982 Origin of the boundary-layer separation on a rotating cylinder in the flow of an incompressible fluid. *Trudy TsAGI* **13** (6), 32–39.

RILEY, N. 1975 Unsteady laminar boundary layers. *SIAM Rev.* **17**, 274–297.

RUBAN, A. I. 1981 Singular solution of the boundary-layer equations which can be extended continuously through the point of zero surface friction. *Izv. Akad. Nauk. SSSR, Mekh. Zhidk. i Gaza* **6**, 42–52.

RUBAN, A. I. 1982*a* Asymptotic theory of short separation regions on the leading edge of a slender airfoil. *Izv. Akad. Nauk. SSSR, Mekh. Zhidk. i Gaza* **1**, 42–51.

RUBAN, A. I. 1982*b* On stability of preseparating boundary layer on the leading edge of a slender airfoil. *Izv. Akad. Nauk. SSSR, Mekh. Zhidk. i Gaza* **6**, 55–63.

RUBAN, A. I. 1990 Marginal separation theory. In *Separated Flows and Jets, Proc. IUTAM Symp.*, pp. 47–54. Springer.

SMITH, F. T. 1982*a* On the high Reynolds number theory of laminar flows. *IMA J. Appl. Maths* **28**, 207–281.

SMITH, F. T. 1982*b* Concerning dynamic stall. *Aeronaut. Q.* **33**, 331–352.

SMITH, F. T. 1984 Concerning upstream influence in separating boundary layers and downstream influence in channel flow. *Q. J. Mech. Appl. Maths* **37**, 389–399.

SMITH, F. T. 1986 Steady and unsteady boundary-layer separation. *Ann. Rev. Fluid Mech.* **18**, 197–220.

SMITH, F. T., BRIGHTON, P. W. M., JACKSON, P. S. & HUNT, J. C. R. 1981 On boundary layer flow past two-dimensional obstacles. *J. Fluid Mech.* **113**, 123–152.

SMITH, F. T. & ELLIOTT, J. W. 1985 On the abrupt turbulent reattachment downstream of leading-edge laminar separation. *Proc. R. Soc. Lond.* A **401**, 1–27.

SMITH, F. T. & WALTON, A. G. 1989 Nonlinear interaction of near-planar TS waves and longitudinal vortices in boundary-layer transition. *Mathematika* **36**, 262–289.

STEWARTSON, K. 1958 On Goldstein's theory of laminar separation. *Q. J. Mech. Appl. Maths* **11**, 399–410.

STEWARTSON, K. 1974 Multistructured boundary layers on flat plates and related bodies. *Adv. Appl. Mech.* **14**, 145–239.

STEWARTSON, K., SMITH, F. T. & KAUPS, K. 1982 Marginal separation. *Stud. Appl. Maths* **67**, 45–61.

STUART, J. T. 1963 In *Laminar Boundary Layers* (ed. L Rosenhead), chap. IX. Oxford University Press.

SYCHEV, V. V. 1980 On certain singularities in solutions of the equations of boundary layer on a moving surface. *Prikl. Matem. Mekh.* **44**, 831–838.

SYCHEV, V. V. 1987 Singular solution of the boundary-layer equations on a moving surface. *Izv. Akad. Nauk. SSSR, Mekh. Zhidk. i Gaza* **2**, 43–52.

SYCHEV, V. V., RUBAN, A. I., SYCHEV, V. V. & KOROLEV, G. L. 1987 *Asymptotic Theory of Separated Flows.* Nauka, Moscow.

TELIONIS, D. P. 1981 *Unsteady Viscous Flows.* Springer.

TELIONIS, D. P. & WERLE, M. J. 1973 Boundary-layer separation from downstream moving boundaries. *Trans. ASME J. Appl. Mech.* **40**, 369–374.

TIMOSHIN, S. N. 1988 Removal of marginal separation in a pulsatile flow. *Prikl. Matem. Mekh.* **52**, 77–81.

TIMOSHIN, S. N. 1995 On short-wavelength instabilities in three-dimensional classical boundary layers. *Eur. J. Mech.* B/*Fluids* **14**, 409–437.

TIMOSHIN, S. N. & SMITH, F. T. 1995 Singularities encountered in three-dimensional boundary layers under an adverse or favourable pressure gradient. *Phil. Trans. R. Soc. Lond.* A **352**, 45–87.

WALTON, A. G. & SMITH, F. T. 1992 Properties of strongly nonlinear vortex/Tollmien-Schlichting-wave interactions. *J. Fluid Mech.* **224**, 649–676.

WILLIAMS, J. C. 1977 Incompressible boundary-layer separation. In *Ann. Rev. Fluid Mech.* **9**, 113–144.

ZAMETAEV, V. B. 1987 Singular solution of the boundary-layer equations on a slender cone. *Izv. Akad. Nauk. SSSR, Mekh. Zhidk. i Gaza* **2**, 65–72.

ZAMETAEV, V. B. 1989 Formation of singularities in a three-dimensional boundary layer. *Izv. Akad. Nauk. SSSR, Mekh. Zhidk. i Gaza* **2**, 58–64.